PCCP

Accepted Manuscript

ROYAL SOCIETY OF CHEMISTRY

www.rsc.org/pccp

ARTICLE TYPE www.rsc.org/xxxxxx | XXXXXXXX

Do adsorbed drugs to P-glycoprotein influence its efflux capability?

Ricardo J. Ferreira[a] ,Maria-José U. Ferreira[a] and Daniel J.V.A. dos Santos[b]*

Received (in XXX, XXX) Xth XXXXXXXXX 200X, Accepted Xth XXXXXXXXX 200X
First published on the web Xth XXXXXXXXX 200X
DOI: 10.1039/b00000000x

The membrane biophysical aspects by which multidrug resistance (MDR) relates with ABC transporters function still remain largely unknown. Notwithstanding the central role that efflux pumps like P-glycoprotein have in MDR onset, experimental studies classified additionally the lipid micro-environment where P-gp is inserted as determinant for the increased efflux capability demonstrated in MDR cell lines. Recently, a nonlinear model for drug-membrane interactions showed that, upon drug adsorption, long-range mechanical alterations are predicted to affect the P-gp ATPase function at drug external concentrations of ~10-100 μM. However, our results also show that drug adsorption may also occur at P-gp nucleotide-binding domains where conformational changes driving efflux takes place. Thus, we assessed the effect of drug adsorption to both protein-water and lipid-water interfaces, by means of molecular dynamics simulations. The results show that free energies of adsorption are lower for modulators in both lipid/water and protein/water interfaces. Important differences in drug-protein interactions, protein dynamics and membrane biophysical characteristics were observed between the different classes. Therefore, we hypothesize that drug adsorption to the protein or lipid-water interface account for a complex network of events that affect the transporters' ability to efflux drugs.

Introduction

One of the major challenges to cancer treatment is multidrug resistance (MDR) presented by cancer cells as a way to surpass the pharmacological action of many chemotherapeutic agents, often structurally unrelated and with distinct mechanisms of action.[1] MDR, in spite of being a multifactorial phenomenon, is thought to be related mostly with the over-expression of ATP-dependent efflux pumps– ABC transporters– at the surface of cancer cells. From the 49 ABC transporters known to exist in the human genome, Multidrug Resistance-associated Protein 1 (MRP1, ABCC1), Breast Cancer Resistance Protein (BCRP, ABCG2, also known as mitoxantrone resistance protein) and P-glycoprotein (P-gp, ABCB1) are the efflux triad mostly reported as being involved in MDR phenomenon.[2–4] Recently, experimental evidences also implied ABCB5, largely expressed in cancer stem cells and malignant melanomas, in the development of MDR phenotype.[5–7]

P-gp, one of the most studied ATP-dependent efflux pumps associated to MDR, is organized in two functional units linked by a polypeptidic sequence with a pseudo two-fold molecular symmetry. Each unit comprises six transmembrane (TM) domains and one cytoplasmic nucleotide-binding domain (NBD) where ATP binds.[8,9] It is widely accepted that the P-gp efflux mechanism involves a hydrophobic vacuum cleaner model[10,11] in which substrates, according to their partition coefficient, accumulate within the lipid bilayer and are translocated from the inner leaflet towards the extracellular space[12–14] or into the outer leaflet.[1,11] P-gp is also characterized by a large internal drug-binding pocket[8] where, at least, three drug-binding sites were identified and characterized.[8,15,16] Many theoretical and experimental studies have been performed in an attempt to clearly identify features associated to substrate recognition and those responsible for efflux modulation. While earlier studies identified nitrogen atoms, aromatic moieties, water/octanol partition coefficient (log*P*) and hydrogen-bond acceptors as important for recognition,[17–21] more recent studies pointed out the presence of tertiary amines, alkoxy groups or sugar moieties as specific efflux promoters– effluxophores.[22] Oppositely, molecules that can modulate P-gp efflux are characterized to be structurally elongated and to have aromatic moieties. Optimal distances between hydrophobic, hydrogen bond donor and acceptor groups are also described to be important for efflux modulation as these moieties increase the probability of establishing π-π, CH-π or hydrogen-bonds with residues inside the drug-binding pocket.[23] Nonetheless, optimal log*P* values are always required to allow higher partition rates towards the lipid bilayer.[24]

The above studies were specifically designed to better understand the interaction between molecules and hypothetical drug-binding sites located at the transmembrane domains inside the lipid bilayer. However, in order to reach these specific locations, any molecule should first diffuse into the lipid bilayer in order to gain access to one of the 'entrance' gates located between TM helices 4/6 or 10/12.[8,25,26] Recently, Rauch *et al.* proposed a physical model by which mechanical interactions between drugs and lipid membranes could directly affect efflux.[27] More specifically, changes on membranes' biophysical properties due to drug adsorption are expected to have an impact on P-gp dependent efflux through a non-linear effect. Namely, membrane energy changes are correlated with drug accumulation as a function of their physico-chemical properties and external concentration in solution. In addition, and as P-gp displays a two-stage curve

for the ATPase activity in the presence of low (increase in activity) or high (decrease in activity) drug concentrations, it was also assumed that drug concentrations are related to P-gp ATPase function and that a range of concentrations would block P-gp in a predetermined state dependent on membrane changes.[27] Hence, the amount of drug needed to effectively block ~50% of P-gp function was estimated between 8-80 μM, in agreement with other experimental studies.[28] Drug permeation towards the lipid bilayer initiates with its adsorption at the water/lipid interface, followed by drug diffusion into the membranes' inner leaflet and, as pointed out by Rauch *et al.*, may account for mechanical changes in the membrane that may have a direct impact on P-gp efflux. Likewise, it is also expected to occur drug adsorption to the cytoplasmic nucleotide-binding domains that might have an impact in the ATP-driven rigid-body motions that drive conformational changes towards substrate efflux. Thus, the efflux model described above implies that P-gp and the lipid bilayer act as a combined entity rather than two independent structures. This is supported by experimental data that identified lipid composition[13,29] and passive permeation rates[29–31] as critical for efflux to occur. Although the previous study by Rauch *et al.* only considered drug-membrane interactions, drug-protein interactions must also occur as a step-by-step addition dependent on law of mass action, in accordance with the thermodynamics of adsorption of small molecules by proteins.[32,33] Molecular dynamics (MD) studies clarified that, for efflux to occur, both NBD domains must induce conformational changes through rigid-body motions around a central pivotal motif that are transmitted to the transmembrane domains (TMDs) by short helical domains located in the intracellular coils (ICLs) at the NBD-TMD interface.[34–37] Thus, as the NBDs account for almost all of P-gp's solvent accessible area, it can be expected that this stepwise adsorption could have some degree of impact on the rigid-body motions that initiate efflux, depending on the number of adsorbed molecules and their physicochemical properties. Moreover, and taking into account that P-gp is a polyspecific efflux pump, the estimation of the drug adsorption free energy towards the transporter and membrane or changes in normal motion patterns may become new suitable molecular descriptors to characterize the efflux susceptibility of molecules commonly described as non-substrates, substrates and modulators.[38]

As stated above, MD studies are increasingly contributing to the knowledge on efflux mechanism by ABC transporters.[38] Computational studies have been used to estimate the interactions and adsorption free energies of peptides[32,39,40] or small molecules[41,42] with several surfaces or lipid bilayers.[43,44] This technique was also successfully used to evaluate cooperative adsorptions at the vacuum-water interface.[45] Therefore, molecular dynamics simulations can also be used to estimate the free energies of adsorption of small molecules towards P-gp and lipid bilayer.

In this paper, a series of molecular dynamics runs comprising twelve small molecules are described, eleven of which are frequently characterized as *non-substrates* (three), *substrates* (five) and *modulators* (three). Adenosine triphosphate (ATP) was also evaluated as the natural substrate for the ATP-binding site located at the canonical dimer interface. The main objectives are, for the first time, to evaluate the free energies of adsorption for molecules of the different groups by 1) identifying the amino acid residues more frequently involved in drug adsorption and 2) to identify mechanical alterations in the bilayers' physical properties derived from drug adsorption at the lipid-water interface. The study of these two properties should provide direct information about the possibility of each class of molecules to interfere with P-gp conformational changes and therefore to have a direct impact in the efflux cycle.

Methods

Initial structures. From a previous study,[25] a system comprising P-gp that also contains an important sequence for drug recognition and ATP hydrolysis[46] inserted in a lipid bilayer with 464 molecules of 1-palmitoyl-2-oleoylphosphatidylcholine (POPC), solvated with 55.896 waters and neutralized with 26 chlorine ions in a total of 204.260 atoms was used as a starting point for free energy calculations. POPC force field parameterization was retained from previous simulations.[47,48] Ligand molecules were parameterized according to the 53a6[49,50] parameter set of GROMOS96[51,52] force-field using the ATB[53–55] or PRODRG[56] on-line servers and manually curated. Mülliken partial charges[57] were assigned through *ab initio* calculations at the Hartree−Fock level of theory using the 6-31G basis set with diffuse (neutral) or diffuse/polarization (charged molecules) functions in the Gaussian03[58] program.

Simulation Parameters. The GROMACS 4.6.x simulation packages[59–63] were used for the MD simulations. All simulations applied periodic boundary conditions (PBC). Initial energy minimizations were performed using the steepest descent method. All *NpT* runs used the Nosé-Hoover [64,65] thermostat and the Parrinello-Rahman[66] barostat for temperature (303 K) and pressure coupling (1 bar), respectively. In the presence of membranes, the pressure equilibration was achieved through a semi-isotropic pressure coupling, with system compressibility defined as 4.5×10^{-5} bar^{-1} and initial box with dimensions *xyz* of 12.75 x 12.75 x 16.55 nm^3. Particle Mesh Ewald (PME) method with cubic interpolation[67,68] and FFT grid spacing of 0.16 was used for long-range electrostatics, with identical short-range cut-off radius for electrostatic and van der Waals interactions (10 Å). Group-based or Verlet[69] cut-off schemes were applied for the calculation of non-bonded interactions on CPU and GPU respectively. SETTLE[70] (for water molecules) or LINCS[71,72] algorithms were used to constrain all bond lengths.

Adsorption Runs. In order to determine the free energy of adsorption of the molecules toward P-gp cytoplasmic domains or lipid bilayer, four different groups were defined based on the classification of Polli *et al.*[73] (later modified by Rautio *et al.*[74]) and Didziapetris *et al.*[75]: alprenolol[75], diphenhydramine[76,77] and ranitidine[78,79] (*non-substrates*); verapamil,[80] colchicine,[81] Rhodamine-123,[82,83] Hoechst 33342,[84] and trimethoprim[85] (*substrates*); latilagascene D,[86,87] tariquidar[88] and the flavonoid kaempferide[89] (*modulators*).

Colchicine, latilagascene D, kaempferide and trimethoprim were considered to be neutral at physiological pH (based on the pK_a values of ionizable groups calculated in MarvinSketch[90]). Another system solely for ATP adsorption was analysed separately. In each system, sixteen molecules (corresponding to concentrations around ~15 μM) were randomly placed in the bulk solvent around the cytoplasmic NBD domains and all water molecules, within 2 Å from each inserted molecule, were removed (with tcl/tk scripting in Visual Molecular Dynamics, VMD)[91]. All systems were then energy minimized, followed by a 50 ns unrestricted *NpT* run. For sampling purposes, two other systems, one containing Hoechst 33342 and the other tariquidar, and three systems for kaempferide were built. Finally, for comparison purposes, the *apo* system MD simulation described in a previous paper[25] was extended for an additional 50 ns.

Data analysis. The trajectories of each molecule that adsorbed either to the NBD domains or the lipid-water interface were used to estimate the free energy of adsorption of the molecules. For protein adsorption, the normalized probability density (P_i) was obtained with *g_rdf* as a radial distribution function for the center of mass densities of a molecule *A* at a distance *r* around the closest atom in *B* (i.e. protein surface). Similarly, for lipid adsorption, and taking into account that the lipid bilayer is similar to a flat surface where molecules adsorb,[39] P_i was obtained in three steps. First, *g_traj* tool was used to extract the *z* coordinate for the center of mass of a given molecule as a function of time. Then, the probability distribution function for each molecule to be at a certain distance from the lipid bilayer in the MD run was determined by first splitting the obtained plot in several bins (Δr = 0.05 Å) and calculating the frequency f_i of a molecule in each bin. Finally, from the positional probability p_i obtained by the equation

$$p_i = \frac{f_i}{\sum f_i}, with \sum p_i = 1 \quad (1)$$

it was possible to calculate the normalized probability density P_i as the quotient between the positional probability (p_i) and bin width (Δr),

$$P_i = \frac{p_i}{\Delta r}, with \sum p_i.\Delta r = 1 \quad (2).$$

The obtained distributions (for each adsorbed molecule) were the basis for the calculation of the free energies of adsorption to the protein or to the lipid through the probability ratio method.[39,92] For each molecule considered, the relative free energy difference (ΔG_i) between two positions was calculated as

$$\Delta G_i = G_i - G_0 = -RT.\ln\left[\frac{P_i}{P_0}\right] \quad (3)$$

where *R* is the ideal gas constant, *T* the absolute temperature (303 K) and G_0 is the free energy of a reference state. For the protein adsorption calculations, the reference state was obtained using the values in bulk water at 20 Å from the interfaces. When adsorption was fast, this cut-off was reduced to 10 Å due to lack of statistics for distances larger than this value (the molecules moved rapidly towards the interface with low probability to be found at larger distances).

Finally, the overall free energy of adsorption for a given molecule was calculated from the weighted sums of the relative free energies,

$$\Delta G_{ads} = \int_{bin} P_i.\Delta G_i.\Delta r \quad (4).$$

Hydrogen-bond and non-bonded interactions between adsorbed molecules and protein residues were evaluated using *g_hbond*[93] and *g_contacts*[94] tools. For each class, the spatial distribution of molecules around P-gp was calculated with *g_spatial* tool available in GROMACS, after centering the protein and removing its periodicity, and rotational and translational motions.

Membrane leaflets are herein identified as upper and lower leaflets, with the lower leaflet being the one close to the nucleotide-binding domains (i.e. cytoplasmic leaflet). Membrane biophysics were characterized by means of area per lipid (A_L) and thickness (D_{HH}) and free energy calculations (ΔG_{def} and ΔG_{res}). A_L and D_{HH} were obtained from the last 10-ns trajectory, when the large majority of the molecules are already adsorbed to the membrane. This was accomplished by extracting a 6x6 nm² bilayer section around the geometrical center of each molecule, using python scripts developed in-house and *trjconv* tool, in order to create suitable input files for GridMAT-MD[95] calculations. Internal drug-binding pocket volume variations as a function of time were calculated using VOIDOO[96,97] software with a 1.2 Å probe radius and a primary grid size of 0.7 Å. For each class of molecules, the P-gp pocket volume probability distribution was obtained by calculating the frequency that each instantaneous value felt in bins of size 100 Å³. Free-energy studies on membrane-deformation energy penalty (ΔG_{def}) and residual hydrophobic exposure energy penalty (ΔG_{res}) were calculated through the hybrid Continuum-Molecular Dynamics (CTMD) approach using CTMD[98] software. Statistical results were performed using the Student's *T-Test* in Libreoffice Calc.

Results

Free energy calculations. The free energy of adsorption for several classes of molecules[71-73] (Chart 1) towards the protein surface and lipid-water interface was assessed. From Figure 1 (and Figure S1 for each molecule individually), it is possible to observe that, in all classes, molecule adsorption is an energetically favourable process. To this matter, the lowest energies were found for ATP in both protein (-9.6±0.6 kJ.mol^{-1}) and membrane (-12.4±1.6 kJ.mol^{-1}) interfaces. However, this can be explained by its negative charge (net charge of -4) that promotes electrostatic interactions with positively charged residues as lysines and arginines or positively charged moieties as cholines (in POPC). However, a statistically significant difference could be found between ATP and all

classes but *modulators* ($p < 0.05$).

Interestingly, *modulators* free energies of adsorption were found to be the lowest among the three evaluated classes, with ΔG_{ads} ranging from -8.8±0.8 kJ.mol^{-1} (protein) up to -9.9±0.5 kJ.mol^{-1} (lipid interface) and also showing a statistically significant difference from *substrates* and *non-substrates* for protein adsorption ($p < 0.05$).

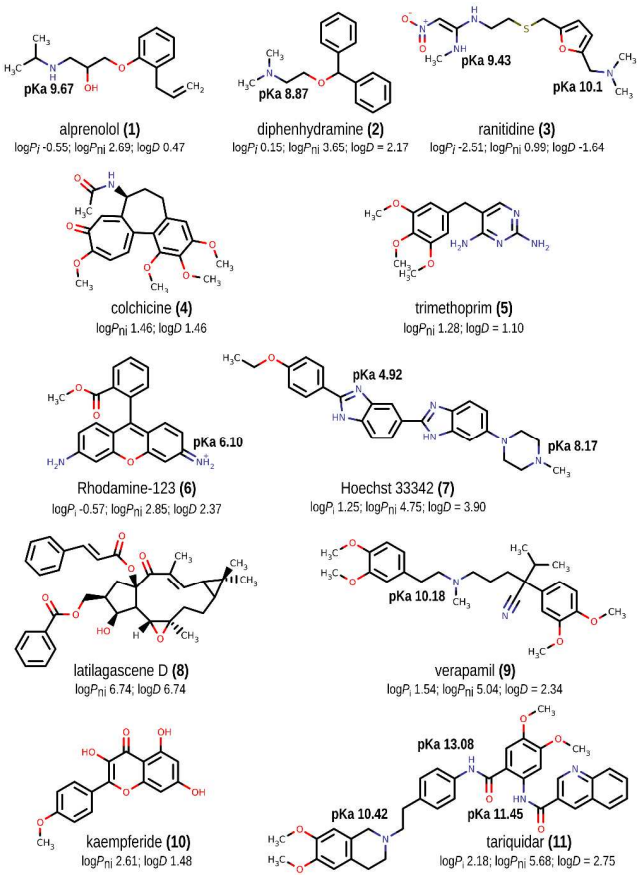

Chart 1. Chemical structures of the molecules used in the MD simulations, with pKa of the ionizable groups, log*P* and log*D* (as calculated by MarvinSketch[90]).

For *substrates* and *non-substrates*, the free energies of binding to each interface were higher than *modulators* but still favourable, as shown in Figure 1 i.e. the calculated free energies of adsorption for *substrates* were -7.1±0.4 kJ.mol^{-1} and -8.9±0.8 kJ.mol^{-1} for the protein and lipid interfaces, whereas for *non-substrates* the calculated energies for each one of the interfaces were -6.0±1.0 and -9.1±2.7 kJ.mol^{-1} respectively.

The adsorption energies towards the lipid-water interface are always more favourable than the ones reported for protein-water interface, suggesting that the adsorption to the lipid bilayer is the primary mode of action for these molecules, in comparison to the adsorption towards P-gp. Moreover, the energetic difference between both interfaces seem to increase from *modulators* (~1.1 kJ.mol^{-1}) to *substrates* (~1.8 kJ.mol^{-1}) and *non-substrates* (~3.1 kJ.mol^{-1}).

It is also worth noticing that drug adsorption to both structures showed different behaviours. When considering molecule adsorption to the protein-water interface, a higher number of molecules are found for both substrates and modulators when compared with non-substrates (Table S1, Supporting Information). Regarding the lipid interface, a close inspection of the *z* coordinate evolution with time (the molecules' path, as obtained by *g_traj*) showed that in few cases (~10%) a transient adsorption of the molecule to the lipid bilayer first occurs before it becomes fully adsorbed. Oppositely, the molecules' adsorption to the protein occurs immediately after the first contact.

In this study, smaller molecules as trimethoprim, diphenhydramine or alprenolol were found to be inserted between the lipid headgroups. However, only kaempferide and diphenhydramine were able to show full permeation into the inner leaflet of the membrane, with one kaempferide molecule additionally showing spontaneous flip-flop between both membrane leaflets. This is found to be in agreement with experimental evidences found for related molecules.[99,100] In addition, it is also known that a wide range of flavonoids bind to vicinal ATP- and steroid-binding sites,[89] modulating efflux by impairing ATP binding. Thus, high adsorption rates were expected for kaempferide that may be related with its modulating activity, not only at the ATP-binding site but also by changing the biophysical properties of membranes.

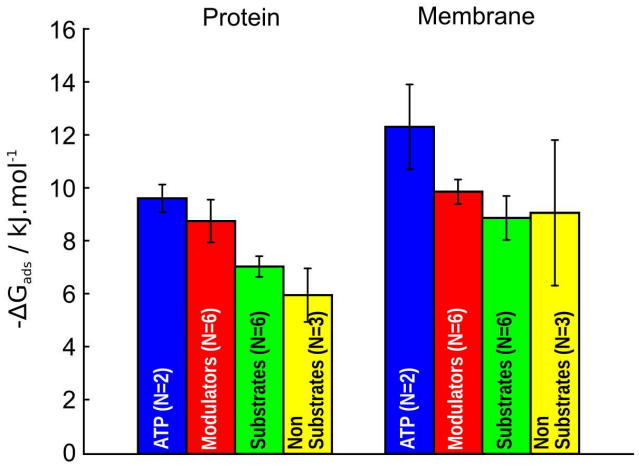

Figure 1. Free energies of adsorption (mean ± SE) for the different classes at protein-water or membrane-water interface. Statistical significance was determined by comparing the different classes with multiple *T-Tests* ($p < 0.05$).

Since several experimental studies clearly demonstrated that molecules may interact with P-gp and induce ATPase activity without significant efflux,[74,76,101] this led us to suppose that a different mechanism, unrelated with substrate competition or passive permeation rates, may also be involved in efflux modulation. In this mechanism, drug adsorption at the surface of NBDs may be able to disturb the mass/charge balance between both domains, affecting the normal motion patterns that drive conformational changes during the efflux cycle. This is in agreement with the observations by Litman *et al.*, showing that the intrinsic affinity of some drugs for the cytoplasmic P-gp surface is four-fold higher than at the other side of the membrane.[102] Moreover, Äanismaa *et al.* also concluded that, at sufficiently high drug concentrations, the P-

gp ATPase works in an enthalpy-driven manner probably due to the loss of residual motion of the transporter.[103]

As suggested by the calculated adsorption energies, NBDs may also participate in the efflux process by increasing the concentration in the surrounding environment, displacing molecules from the bulk water environment into the water shell next to their surface, which may indirectly also enhance membrane permeation. In addition, drug adsorption may also affect the normal motion patterns. This effect may respond to changes in the surrounding environment, with the magnitude of such changes intimately related with the physico-chemical properties of the adsorbed molecules.

Protein interaction profile. We thoroughly investigated all interactions between individual molecules that effectively adsorbed to the protein (Table 1) or to the lipid bilayer.

Table 1. Contacts and hydrogen bond statistics for each class of molecules. $<N_{NB}>$, average number of non-bonded interactions per class; ARO, interaction with aromatic residues; HYD, interaction with hydrophobic residues; POL, interaction with polar residues; $<N_{HB}>$, average number of hydrogen bonds per time frame; $<\tau>$, mean hydrogen bond lifetime; ΔG_{HB}, HB formation energy in kJ.mol^{-1}.

	Interaction type						
	Contacts				Hydrogen bonds		
Classes	$<N_{NB}>$	ARO %	HYD %	POL %	$<N_{HB}>$	$<\tau>$ ps	ΔG_{HB} kJ.mol^{-1}
non-substrates	7.8	13.7	23.4	62.8	0.47	1035	-20.9
substrates	8.6	10.8	33.6	55.6	0.85	1631	-22.4
modulators	16.6[a]	9.7	26.8	63.5	1.09	1481	-22.3
ATP	11.1	12.3	16.3	71.4	2.82[b]	2351[c]	-23.9[b]

Statistical significance was determined by comparing the different classes with multiple t-Tests ([a], $p < 0.05$ with *non-substrates* and *substrates*; [b], $p < 0.05$ with *non-substrates*; [c], $p < 0.05$ with all classes). Data for individual molecules are is available in Figures S3-S5).

While for membrane adsorption electrostatic interactions play a major role due to the charged phosphate and choline moieties at the lipid headgroups, protein adsorption seems to be not only dependent on negatively (glutamate, aspartate) and positively charged (lysine, arginine) residues but also on hydrogen-bond donor residues such as glutamine and asparagine. Interestingly, all classes seem to preferentially interact with residues with additional methylenic units (-CH_2-) like glutamate and glutamine (against aspartate and asparagine) or even longer sidechains as in arginine and lysine (with two and three additional methylenic units respectively). In addition, from Table 1 a sustainable increase in the total number of interactions occurs from *non-substrates* toward *modulators*.

Regarding protein contacts, *substrates* interaction pattern is higher for hydrophobic residues when compared with the other classes, also showing fewer interactions with polar residues. Oppositely, *modulators* interaction with aromatic residues is always lower when compared with the remaining classes, leading us to assume that polar interactions have a greater importance for the molecules included in this class. As expected, ATP interacts mainly through electrostatic and/or hydrogen bond interactions and higher contact frequencies with polar residues were effectively observed throughout the simulation time.

For hydrogen bond (HB) capability, it is also possible to see that the mean number of hydrogen bonds per time frame also increases from *non-substrates* (0.47) to *modulators* (1.09). While *non-substrates* have the highest HB formation energies (ΔG_{HB}, -20.9 kJ.mol^{-1}), all the remaining classes have similar energies around -22.3±0.1 kJ.mol^{-1}. However, higher hydrogen bond lifetimes are registered for *substrates* (1631 ps) when compared with *modulators* (1481 ps) and even higher than for *non-substrates* (1035 ps). Finally, ATP registered the highest number of HB per time frame (2.82) and HB lifetimes (2351 ps) and the lowest ΔG_{HB} values (-23.9 kJ.mol^{-1}).

The electrostatic contribution to drug adsorption was also assessed by comparing the relative interaction free energies between neutral and charged molecules with P-gp during the last 10 ns of each simulation. In this case, since P-gp is a transmembrane protein, a correction to the polar solvation energy must be taken into account due to the presence of a membrane. To this matter, we applied an implicit membrane correction by generating ion-accessibility and dielectric maps incorporating the membrane environment, in which the dielectric slab constant is set to 2.0 by the *draw_membrane2* program (obtained from www.poissonboltzmann.org), to obtain the corrected polar solvation energies able to be used as input with *g_mmpbsa*[104] tool available for GROMACS.

From the obtained energies by the above method (Figure S2), two distinct behaviours were observed. While *non-substrates* interaction energies were similar within the group, for both *substrates* and *modulators* the interaction energy decreased almost linearly with increasing molecular size, in agreement other published reports.[105,106] Thus, an efficiency index (EI) was calculated by dividing each interaction energy by the molecules' molecular weight (MW) to assess possible differences between charged and neutral molecules (Table 2).

Table 2. Comparison between neutral and charged molecules on protein adsorption

Efficiency Index (EI)				
non-substrates (charged)	*substrates (neutral)*	*substrates (charged)*	*modulators (neutral)*	*modulators (charged)*
0.22±0.06 [b]	0.07±0.02 [a]	0.17±0.04	0.06±0.02 [a]	0.15±0.03

Statistical significance was determined with t-Tests ([a], $p < 0.05$ between charged and neutral molecules within the same class; [b], $p < 0.05$ with all groups except *charged substrates*).

From Table 2, it is possible to conclude that charged molecules have higher efficiency indexes when compared with neutral ones, implying that electrostatic interactions, together with hydrogen bonding, are important for drug adsorption.

Based on the findings described above, small molecules' adsorption to the protein surface seem to be highly influenced by electrostatics and hydrogen bonding. Thus, hydrogen bond capability and electrostatics can be significant in defining the strength of the adsorption by increasing molecules' residence time at the protein surface, contributing this way for a greater stabilization of the ligand-protein complex. As many

molecules are found to be simultaneously adsorbed to the protein surface, changes on the mass/charge relation between NBDs may be susceptible to perturb the proteins residual motion patterns, as previously suggested by Äanismaa *et al.*.[103]

Additionally, by generating spatial distribution maps, adsorption preferences on specific regions around nucleotide-binding domains (NBDs) were also evaluated for all classes (Figure 2).

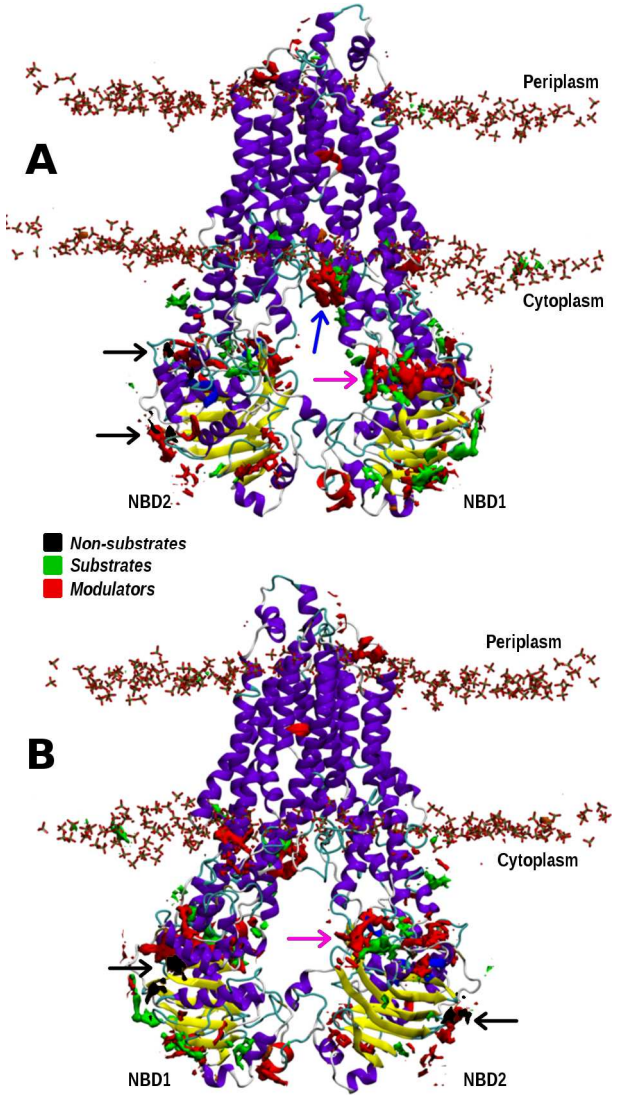

Figure 2. Spatial distribution maps for the different classes. A. Front view; B, Back view. Isosurfaces represent a probability greater than 50% of molecules to be located in that particular region. Phosphate groups are also represented to assess lipid-water interface boundaries.

It is worth noticing that *non-substrates* are characterized by weak population densities around the protein, most of which located on coil motifs next to α-helix or β-sheet motifs (black arrows). All other classes show higher densities next to both NBDs, with *substrates* achieving higher densities next to β-sheets and modulators around α-helices and coils. Interestingly, both *substrates* and *modulators* show increased densities around both TMD-NBD interfaces (pink arrows), next to intracellular helices (ICHs) thought to mediate the transmission to the transmembranar domains of conformational changes triggered by ATP binding/hydrolysis. Moreover, higher densities were also found for *substrates* and *modulators* at the lipid-water interface (blue arrow), next to one of the hypothetical 'entrance gate' located between TMDs 4 and 6.

From the above spatial distribution maps, the adsorption of molecules to these specific locations may perturb the transmission of normal motions induced by ATP binding to the transmembranar domains (TMD-NBD interfaces) or may promote drug permeation into the membrane in order to be effluxed by P-gp (when at the lipid-water interface next to 'entrance gates'). To our knowledge, only another study identified the TMD-NBD interface as a possible interaction region for substrates.[107] In addition, these results are also in agreement with a recently published MD study[108] and provides new insights on the different adsorption patterns between *non-substrates*, *substrates* and *modulators*.

Internal cavity volumes. In a previous paper we also demonstrated that a better helix repacking due to membrane and linker insertion were important for stabilizing the volume of the internal drug-binding pocket around 4000 Å³.[25] As the above results indicate that drug adsorption occurs in specific locations that may affect residual motion patterns, to evaluate the impact that drug adsorption may have on helix repacking of the transmembrane domains we monitored the internal cavity volume throughout the simulation time (Figure 3) to allow a better comparison of the volume variations associated to each class.

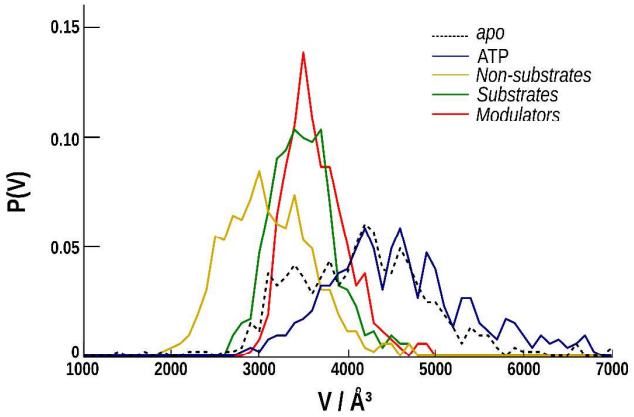

Figure 3. Normalized internal cavity volume distributions for the *apo* structure and the different classes.

In the presence of ATP, the volume distribution is almost identical to the values registered for the *apo* structure, supporting the fact that ATP adsorption either to the membrane or to the protein surface was not able to induce significant alterations in the TMD packing. However, with *non-substrates* the volume distribution is shifted to lower volumes (2100-4000 Å³) than the ones registered for the *apo* system (2900-5600 Å³). In this case, the number of molecules adsorbed to the lipid-water interface is higher than to the protein-water interface and the correspondent adsorption energies are also more favourable. In addition, the large majority of the adsorbed molecules are located below the choline moiety, next to the phosphate groups. This class has

protonated nitrogen atoms and a molecular weight below 400 kDa that favours adsorption to the lipid bilayer. Therefore, for *non-substrates*, it seems that changes in the volume of the internal drug-binding pocket respond to modifications in membrane properties rather than protein motions.

Similarly, *substrates* and *modulators* also shift down volumes regarding the *apo* system, although in a lesser extent. However, they both narrow down the calculated volume distributions to values with maximum probabilities around 3400-3500 Å³ (2700-4700 Å³ and 2900-4900 Å³ interval, respectively). *Substrates* and *modulators* seem to induce a more efficient TMD reorientation/repacking, which can be due to the previously reported interaction with the ICHs at the TMD-NBD interface and enhanced communication between both domains. As already suggested in a previous paper,[38] these data support the hypothesis that targeting the TMD-NBD interface with small molecules able to decouple TMD-NBD motions would affect the coordinated NBD-TMD motions the same way as mutations in the ICH do.[109–111]

Membrane biophysics. Since Rauch *et al.*[27] suggested that mechanical alterations of the lipid bilayer may have a direct impact on P-gp efflux through a non-linear effect, the effect of drug adsorption on the biophysical properties of the membrane was also evaluated. However, no statistically relevant changes were found for standard properties like lateral diffusion, acyl chain order parameters and membrane densities (assessed by *g_msd*, *g_order* and *g_density* tools respectively). Hence, as drug adsorption to membranes are described to induce alterations in the area per lipid (A_L) and membrane thickness (D_{HH}), these properties were additionally calculated for each adsorbed molecule and the results are summarized in Figure 4.

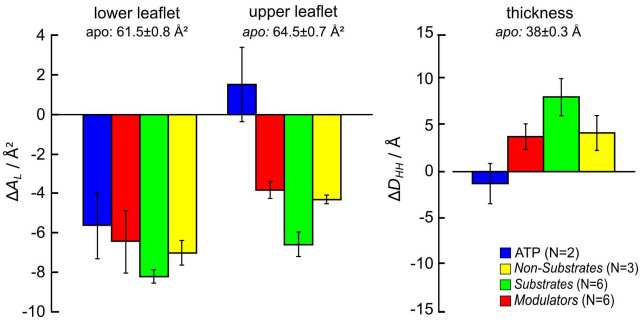

Figure 4. Area per lipid ($\Delta A_L \pm$ SE) and thickness ($\Delta D_{HH} \pm$ SE) variations for each class.

We found that, although no correlation was found between changes in the total area per lipid and the number of adsorbed molecules, adsorbed molecules induce a decrease in A_L values in a 3 nm radius around its geometrical center (Figures S31 to S33). To this matter, all classes decreased A_L values similarly in both the inner (in a greater extent) and outer leaflets, with minimum values being registered for *substrates* with 53.2 Å² and 54.8 Å² for the lower and upper leaflets respectively. As neither charge nor molecular weight seem to affect drug adsorption to the lipid-water interface, the data corroborate the fact by which drug adsorption to membranes occur in a rather unspecific manner. However, the decrease of A_L together with a slight increase in membrane thickness suggests that lipids become more tightly packed, similarly to what is observed in lipid-ordered domains where P-gp is found to be highly active.[14,112–115] The ability of substrates and inhibitors to modify ATPase activity was proved to be higher in the liquid-ordered phase, with lipids tightly packed with cholesterol[116] but still having lateral motility comparable to the liquid-crystalline phase.[117] In addition, large transmembrane P-gp domains are also thought to mediate its association to lipid rafts and to enhance affinity towards cholesterol-enriched domains.[118,119] Thus, if drug adsorption can assist, at least partially, in the formation of such liquid-ordered domains, optimal P-gp activity would be promoted.[114,120]

As P-gp is a multi-helical transmembrane protein with large membrane-spawning domains, membrane deformation to accommodate hydrophobic mismatches is expected to occur. Yet, it is known that P-gp has a large destabilizing effect on the surrounding lipid environment up to 375±197 lipids, equivalent to a 15-20 nm radius around the protein.[114,120] Thus, instead of analysing the protein effect on membrane deformation, we used the Continuum-Molecular Dynamics (CTMD) approach to quantify energetic changes on the membrane biophysics due to drug adsorption.[98] According to this method, the contributions of the membrane deformation energy penalty (ΔG_{def}) and residual hydrophobic exposure energy penalty (ΔG_{res}) were calculated for all ligand systems (Figures S6-S17) and compared with the *apo* system (Figure 5).

Quite surprisingly, only diphenhydramine (*non-substrate*) and kaempferide (*modulator*) increase the energy penalty due to membrane deformation (ΔG_{def}), which may contribute to a destabilizing effect of the transporter (Table 3). Interestingly, both systems were the only ones in which membrane permeation was observed. Thus, the increase of the ΔG_{def} energetic penalty may be correlated with the fact that diphenhydramine and kaempferide were able to fully permeate into the membrane hydrophobic core and with the number of molecules (at least three) that entered the membrane. While other molecules as ranitidine (*non-substrate*), Rhodamine-123, trimethoprim (*substrates*) and tariquidar (*modulator*) seem to have a minimal impact on membrane deformation, all the remaining molecules alleviate the hydrophobic mismatch, with values ranging from -1.44 k_BT for verapamil up to -3.14 k_BT in Hoechst 33342 (both *substrates*).

Table 3. Membrane deformation energy penalty (ΔG_{def}).

		Energetic Penalty (k_BT)
non-substrates	alprenolol	-1.86
	diphenydramine	1.77
	ranitidine	-1.00
substrates	colchicine	-2.09
	Hoechst 33342	-3.14
	Rhodamine-123	-0.03
	trimethoprim	-0.70
	verapamil	-1.44
modulators	latilagascene D	-2.15
	kaempferide	2.09
	tariquidar	-0.05

These results, along with the result obtained from A_L and D_{HH}, reinforces the fact that by inducing a more ordered state the energy penalty associated with membrane deformation decreases due to a better compensation of hydrophobic mismatches. Therefore, drug adsorption to the lipid-water interface may assist the formation of such domains, with implications on the efflux activity of the transporter.

In addition to the above described effect, drug adsorption to either protein-water and lipid-water interface may also contribute to change not only the pattern of membrane deformation but also the residual hydrophobic exposure of residues located at the end of each transmembrane domains. Similar to the results reported for rhodopsin and 5-HT_{2A} receptors,[98,121] P-gp also reveal radially asymmetric deformations around each TMD (Figures S18-S29). Regarding hydrophobic residue exposure, a striking difference emerges between classes. While ATP seem to asymmetrically change the hydrophobic exposure of both *N*-terminal and *C*-terminal domains, both *non-substrates* and *modulators* seem to stabilize the protein by reducing the energetic penalty in both halves. However, this effect is much more pronounced in TMD1 for *non-substrates* whereas in *modulators* the same effect is similarly distributed by all transmembranar helices. Interestingly, *substrates* do not show this behaviour, having a negligible effect on all transmembranar domains except TM helices 1 (decreasing exposure) and 9 (increasing exposure).

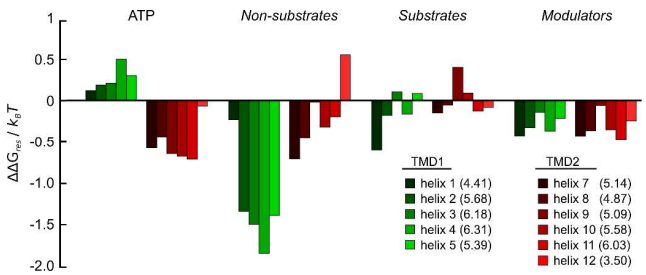

Figure 5. Changes in the residual hydrophobic exposure energy penalty ($\Delta\Delta G_{res}$) for each class compared with the *apo* system (under parenthesis in k_BT units). TMD1, *N*-terminal transmembrane domain; TMD2, *C*-terminal transmembrane domain. Residue exposure for helix 6 in TMD1 was unable to be determined (no exposed residues to the bilayer).

The above data support the fact that mechanical alterations can indeed be induced by drug adsorption to the lipid bilayer interface (with or without permeation) but also to the cytoplasmic domains of P-gp.

Nonetheless, such changes heavily depend on the physico-chemical characteristics of molecules, lipid composition and number of adsorbed molecules. Moreover, it is not totally clear if the observed membrane changes are due solely to drug adsorption at the lipid-water interface or if drug adsorption at the protein-water interface also contributes for changes in the bilayer.

Conclusions

In the last decade, many experimental and theoretical studies identified the transporter-membrane as functional unit and essential for efflux to occur.[24,122-124] More recently, Rauch *et al.*[27] proposed that upon drug binding mechanical alterations in the lipid bilayer are directly responsible for alterations in drug efflux, with such changes linked to physico-chemical properties and external concentration of the drug.

In this paper, using the calculated free energies of adsorption of several molecules towards the protein and lipid bilayer, it was possible to determine that molecules belonging to the *modulators* group are characterized by lower adsorption energies towards nucleotide-binding domains of P-gp and lipid bilayer. When compared with *non-substrates* and *substrates,* this difference was calculated to be statistically significant for protein adsorption. Moreover, in some cases' lipid adsorption was found to be transitory, with the molecule only becoming adsorbed at higher simulation times. Smaller molecules as diphenhydramine and kaempferide were also found to spontaneously diffuse into the membrane, eventually flip-flopping from one leaflet to the other (as observed for kaempferide).

Protein-ligand interactions identified polar residues with the ability to induce the formation of hydrogen bond networks or to participate in electrostatic interactions as the most important factors for drug adsorption. The average contact number per time unit increases in the following order: *non-substrates, substrates* and *modulators,* with amino acids containing longer sidechains like lysine, glutamine or glutamate (-CH_2-CH_2-) being favoured in the interaction with all classes, probably due to CH-π interactions with aromatic rings. Since charged residues as glutamic and aspartic acid (negatively charged) and lysine or arginine (positively charged) residues are also involved in drug adsorption at the NBDs surface, the estimation of molecules' interaction free energies by the MM/PBSA method allowed to conclude that electrostatics, along with hydrogen bonding, play a role for molecule adsorption to the protein surface.

Our study shows differences in density distribution of molecules around the cytoplasmic NBDs, with lower population densities for *non-substrates* when compared with the remaining classes. In the latter, while *substrates* show higher densities around β-sheet motifs, *modulators* revealed higher densities in both α-helices and coil motifs. However, both classes revealed higher spatial distributions in locations around the TMD-NBD interfaces and at the lipid interface next to the 'entrance gate' located between TM helices 4 and 6. If adsorbed to this particular regions, especially at the TMD-NBD interface, normal motion patterns are expected to change due to alterations in how coordinated motion following ATP binding are transmitted to the transmembrane domains.

As the drug-binding site is located in a cavity limited by the membrane-spawning domains, the volume of the internal cavity was also calculated as a function of time. Surprisingly, we found that while ATP adsorption have a negligible effect on the volume probability distribution, molecules from the *non-substrates* class shifts volume distribution of the internal cavity toward lower values. For *substrates* and *modulators*, however, this distribution is narrower and steeper when compared with the *apo* system. This suggests that *substrates*

and *modulators* have a distinct effect on the efflux process when compared with *non-substrates*. Moreover, as both *substrates* and *modulators* adsorbed to the TMD-NBD interface while *non-substrates* do not, such changes in the internal drug-binding pocket volume probably arose from changes in how the NBDs normal motion patterns are transmitted to the transmembranar domains (as suggested above). However, the specific mode of action describing how substrates and modulators can affect the TMD/NBD communication still needs to be further investigated.

On the other hand, molecule adsorption to the lipid bilayer is also expected to change the biophysical behaviour of the membrane through a nonlinear effect.[27] For small molecules having hydrogen-bond acceptor and donor capability, as colchicine, kaempferide or trimethoprim, simultaneous interactions with multiple phospholipids are expected to decrease membrane fluidity, as also described in another study.[125]

Several experimental studies suggested that higher lipid packing within membranes provide optimal P-gp efflux activity.[114,120] Moreover, it is also known that P-gp rearranges the surrounding lipid environment up to a 15-20 nm radius.[120] Herein, all molecules induced a decrease in the calculated area per lipid (A_L) in both leaflets, additionally increasing membrane thickness (D_{HH}) in a lesser extent, which suggests the formation of more liquid-ordered patches around P-gp. Thus, these combined effects would further increase the formation of liquid-ordered domains around P-gp, stimulating the efflux activity proportionally to the number of adsorbed molecules.

Another approach for multi-helical transmembrane protein relies on the evaluation of the quantification of membrane energetic changes due to drug adsorption. By means of CTMD approach, we verified that only molecules that are able to diffuse into the hydrophobic core of the membrane increase the energetic penalty due to membrane deformation (ΔG_{def}), while molecules as colchicine, Hoechst 33342 and verapamil (*substrates*) seem to decrease it. Moreover, *substrates* also seem to have a minimal impact on the calculated hydrophobic residue exposure energy penalty (ΔG_{res}) whereas *non-substrates* and *modulators* seem to have a stabilizing effect by decreasing the energetic penalty ($\Delta\Delta G_{res}$).

It should be noted that classical force fields show some limitations in the evaluation of drug-membrane interactions. For instance, cation-π interactions due to monopole electrostatics based on atomic partial charges cannot be fully described. However, force fields with multipole representation of electrostatics are very time-consuming and a cost-benefit should be weighted while using big biological systems as the ones herein described. Nonetheless, force fields with monopole electrostatics are central in exploring a problem and provide a useful framework for hypothesis generation and testing, regardless of the level of atomic resolution.126 For more accurate predictions, multipole corrections should be applied to classical force fields[127,128] in order to assess particular details of the systems. Alternatively, force fields incorporating multipole electrostatic models that includes polarizability such as AMOEBA[129,130] can also be used for the prediction of such thermodynamic properties.

Notes and references

[a] *Research Institute for Medicines (iMed.Ulisboa), Faculdade de Farmácia, Universidade de Lisboa, Av.Prof. Gama Pinto, Lisboa, Portugal. Fax: +351 217946470; Tel: +351 217946400; E-mail: rjdgferreira@ff.ulisboa.pt; mjuferreira@ff.ulisboa.pt*
[b] *REQUIMTE, Department of Chemistry and Biochemistry, Faculty of Sciences, University of Porto, Rua do Campo Alegre, Porto, Portugal. Fax: +351 220402009; Tel: +351 220402000; E-mail: dsantos@ff.ul.pt*

† Electronic Supplementary Information (ESI) available: [graphical data for individual molecules and membrane-deformation profiles]. See DOI: 10.1039/b000000x/

The authors declare no competing financial interests.
The authors acknowledge Fundação para a Ciência e Tecnologia (FCT, Portugal) for funding (project PTDC/QEQ-MED/0905/2012 and PhD grant to Ricardo J. Ferreira, SFRH/BD/84285/2012).

1 P. D. W. Eckford and F. J. Sharom, *Chem Rev*, 2009, **109**, 2989–3011.
2 R. Callaghan, A. M. George and I. D. Kerr, in *Comprehensive Biophysics*, Elsevier, 2012, vol. 8, pp. 145–173.
3 F. J. Sharom, *Pharmacogenomics*, 2008, **9**, 105–127.
4 G. Szakács, J. K. Paterson, J. A. Ludwig, C. Booth-Genthe and M. M. Gottesman, *Nat Rev Drug Discov*, 2006, **5**, 219–34.
5 T. Kawanobe, S. Kogure, S. Nakamura, M. Sato, K. Katayama, J. Mitsuhashi, K. Noguchi and Y. Sugimoto, *Biochem Biophys Res Commun*, 2012, **418**, 736–741.
6 N. Y. Frank, A. Margaryan, Y. Huang, T. Schatton, A. M. Waaga-Gasser, M. Gasser, M. H. Sayegh, W. Sadee and M. H. Frank, *Cancer Res*, 2005, **65**, 4320–4333.
7 B. J. Wilson, K. R. Saab, J. Ma, T. Schatton, P. Pütz, Q. Zhan, G. F. Murphy, M. Gasser, A. M. Waaga-Gasser, N. Y. Frank and M. H. Frank, *Cancer Res*, 2014, **74**, 4196–4207.
8 S. G. Aller, J. Yu, A. Ward, Y. Weng, S. Chittaboina, R. Zhuo, P. M. Harrell, Y. T. Trinh, Q. Zhang, I. L. Urbatsch and G. Chang, *Science (80-.).*, 2009, **323**, 1718–1722.
9 J. Li, K. F. Jaimes and S. G. Aller, *Protein Sci*, 2014, **23**, 34–46.
10 Y. Raviv, H. B. Pollard, E. P. Bruggemann, I. Pastan and M. M. Gottesman, *J Biol Chem*, 1990, **265**, 3975–3980.
11 C. F. Higgins and M. M. Gottesman, *Trends Biochem Sci*, 1992, **17**, 18–21.
12 A. E. Senior, M. K. Al-Shawi and I. L. Urbatsch, *FEBS Lett*, 1995, **377**, 285–289.
13 I. L. Urbatsch and A. E. Senior, *Arch Biochem Biophys*, 1995, **316**, 135–40.
14 Y. Romsicki and F. J. Sharom, *Biochemistry*, 1999, **38**, 6887–6896.
15 A. B. Shapiro and V. Ling, *Eur J Biochem*, 1997, **250**, 130–137.
16 R. J. Ferreira, M.-J. U. Ferreira and D. J. V. A. dos Santos, *J Chem Inf Model*, 2013, **53**, 1747–1760.
17 H. L. Pearce, A. R. Safa, N. J. Bach, M. A. Winter, M. C. Cirtain and W. T. Beck, *Proc Natl Acad Sci U S A*, 1989, **86**, 5128–5132.
18 J. M. Ford, W. C. Prozialeck and W. N. Hait, *Mol Pharmacol*, 1989, **35**, 105–15.
19 A. Seelig, *Int J Clin Pharmacol Ther*, 1998, **36**, 50–4.
20 R. J. Ferreira, D. J. V. A. dos Santos, M. J. U. Ferreira and R. C. Guedes, *J Chem Inf Model*, 2011, **51**, 1315–1324.
21 M. Reis, R. J. Ferreira, J. Serly, N. Duarte, A. M. Madureira, D. J. V. A. dos Santos, J. Molnár and M.-J. U. Ferreira, *Anticancer Agents Med Chem*, 2012, **12**, 1015–1024.
22 J. Levatić, J. Curak, M. Kralj, T. Smuc, M. Osmak and F. Supek, *J Med Chem*, 2013, **56**, 5691–5708.
23 I. Jabeen, P. Wetwitayaklung, P. Chiba, M. Pastor and G. F. Ecker, *J Comput Aided Mol Des*, 2013, **27**, 161–171.
24 A. T. Clay and F. J. Sharom, *Biochemistry*, 2013, **52**, 343–354.
25 R. J. Ferreira, M.-J. U. Ferreira and D. J. V. A. dos Santos, *J Chem Theory Comput*, 2012, **8**, 1853–1864.
26 R. J. Ferreira, M.-J. U. Ferreira and D. J. V. A. dos Santos, 2015

(submitted).
27 C. Rauch, S. W. Paine and P. Littlewood, *Biochim Biophys Acta*, 2013, **1830**, 5112–8.
28 T. Litman, T. Zeuthen, T. Skovsgaard and W. D. Stein, *Biochim. Biophys. Acta*, 1997, **1361**, 159–68.
29 G. D. Eytan, R. Regev and Y. G. Assaraf, *J Biol Chem*, 1996, **271**, 12897–12902.
30 G. D. Eytan and P. W. Kuchel, *Int Rev Cytol*, 1999, **190**, 175–250.
31 R. Regev, H. Katzir, D. Yeheskely-Hayon and G. D. Eytan, *FEBS Lett*, 2007, **274**, 6204–6214.
32 S. P. Harrold and B. A. Pethica, *Trans Faraday Soc*, 1958, **54**, 1876–1884.
33 A. N. Kuznetsov, B. Ebert, G. Lassmann and A. B. Shapiro, *Biochim Biophys Acta*, 1975, **379**, 139–46.
34 S.-Y. Chang, F.-F. Liu, X.-Y. Dong and Y. Sun, *J Chem Phys*, 2013, **139**, 225102.
35 J. G. Wise, *Biochemistry*, 2012, **51**, 5125–5141.
36 M. Moradi and E. Tajkhorshid, *Proc Natl Acad Sci USA*, 2013, **110**, 18916–18921.
37 J. M. Damas, A. S. F. Oliveira, A. M. Baptista and C. M. Soares, *Protein Sci*, 2011, **20**, 1220–1230.
38 R. J. Ferreira, M.-J. U. Ferreira and D. J. V. A. dos Santos, *WIREs Comput Mol Sci*, 2015, **5**, 27–55.
39 V. P. Raut, M. A. Agashe, S. J. Stuart and R. A. Latour, *Langmuir*, 2005, **21**, 1629–39.
40 M. Mijajlovic, M. J. Penna and M. J. Biggs, *Langmuir*, 2013, **29**, 2919–26.
41 V. Chashchikhin, E. Rykova and A. Bagaturyants, *J Phys Chem Lett*, 2013, **4**, 2298–2302.
42 G. Nawrocki and M. Cieplak, *Phys Chem Chem Phys*, 2013, **15**, 13628–36.
43 M. A. Villarreal, M. Perduca, H. L. Monaco and G. G. Montich, *Biochim Biophys Acta*, 2008, **1778**, 1390–7.
44 X. Yu, Q. Wang, Q. Pan, F. Zhou and J. Zheng, *Phys Chem Chem Phys*, 2013, **15**, 8878–89.
45 S. R. Euston, P. Hughes, M. A. Naser and R. E. Westacott, *Biomacromolecules*, 2008, **9**, 3024–3032.
46 R. J. Ferreira, M.-J. U. Ferreira and D. J. V. A. dos Santos, *Mol Inf*, 2013, **32**, 529–540.
47 D. Poger, W. F. Van Gunsteren and A. E. Mark, *J Comput Chem*, 2010, **31**, 1117–25.
48 D. Poger and A. E. Mark, *J Chem Theory Comput*, 2010, **6**, 325–336.
49 C. Oostenbrink, A. Villa, A. E. Mark and W. F. van Gunsteren, *J Comput Chem*, 2004, **25**, 1656–76.
50 C. Oostenbrink, T. a. Soares, N. F. a Van Der Vegt and W. F. Van Gunsteren, *Eur Biophys J*, 2005, **34**, 273–284.
51 W. R. Scott, P. H. Hünenberger, I. G. Tironi, A. E. Mark, S. R. Billeter, J. Fennen, A. E. Torda, T. Huber, P. Krüger and W. F. van Gunsteren, *J Phys Chem A*, 1999, **103**, 3596–3607.
52 A. M. Bonvin, A. E. Mark and W. F. van Gunsteren, *Comput Phys Commun*, 2000, **128**, 550–557.
53 A. K. Malde, L. Zuo, M. Breeze, M. Stroet, D. Poger, P. C. Nair, C. Oostenbrink and A. E. Mark, *J Chem Theory Comput*, 2011, **7**, 4026–4037.
54 K. B. Koziara, M. Stroet, A. K. Malde and A. E. Mark, *J Comput Aided Mol Des*, 2014, **28**, 221–33.
55 S. Canzar, M. El-Kebir, R. Pool, K. Elbassioni, A. E. Mark, D. P. Geerke, L. Stougie and G. W. Klau, *J Comput Biol*, 2013, **20**, 188–98.
56 A. W. Schüttelkopf and D. M. F. van Aalten, *Acta Crystallogr D Biol Crystallogr*, 2004, **60**, 1355–63.
57 R. S. Mulliken, *J. Chem. Phys.*, 1955, **23**, 1833.
58 M. J. Frisch, G. W. Trucks, H. B. Schlegel, G. E. Scuseria, M. A. Robb, J. R. Cheeseman, J. A. Montgomery Jr., T. Vreven, K. N. Kudin, J. C. Burant, J. M. Millam, S. S. Iyengar, J. Tomasi, V. Barone, B. Mennucci, M. Cossi, G. Scalmani, N. Rega, G. A. Petersson, H. Nakatsuji, M. Hada, M. Ehara, K. Toyota, R. Fukuda, J. Hasegawa, M. Ishida, T. Nakajima, Y. Honda, O. Kitao, H. Nakai, M. Klene, X. Li, J. E. Knox, H. P. Hratchian, J. B. Cross, V. Bakken, C. Adamo, J. Jaramillo, R. Gomperts, R. E. Stratmann, O. Yazyev, A. J. Austin, R. Cammi, C. Pomelli, J. W. Ochterski, P. Y. Ayala, K. Morokuma, G. A. Voth, P. Salvador, J. J. Dannenberg, V. G. Zakrzewski, S. Dapprich, A. D. Daniels, M. C. Strain, O. Farkas, D. K. Malick, A. D. Rabuck, K. Raghavachari, J. B. Foresman, J. V. Ortiz, Q. Cui, A. G. Baboul, S. Clifford, J. Cioslowski, B. B. Stefanov, G. Liu, A. Liashenko, P. Piskorz, I. Komaromi, R. L. Martin, D. J. Fox, T. Keith, M. A. Al-Laham, C. Y. Peng, A. Nanayakkara, M. Challacombe, P. M. W. Gill, B. Johnson, W. Chen, M. W. Wong, C. Gonzalez and J. A. Pople, 2004.
59 H. J. Berendsen, D. van der Spoel and R. van Drunen, *Comput Phys Commun*, 1995, **91**, 43–56.
60 S. Pronk, S. Páll, R. Schulz, P. Larsson, P. Bjelkmar, R. Apostolov, M. R. Shirts, J. C. Smith, P. M. Kasson, D. van der Spoel, B. Hess and E. Lindahl, *Bioinformatics*, 2013, **29**, 845–854.
61 B. Hess, C. Kutzner, D. van der Spoel and E. Lindahl, *J Chem Theory Comput*, 2008, **4**, 435–447.
62 D. Van Der Spoel, E. Lindahl, B. Hess, G. Groenhof, A. E. Mark and H. J. Berendsen, *J Comput Chem*, 2005, **26**, 1701–18.
63 E. Lindahl, B. Hess and D. van der Spoel, *J Mol Model*, 2001, **7**, 306–317.
64 S. Nosé, *Mol Phys*, 2002, **100**, 191–198.
65 W. Hoover, *Phys Rev A*, 1985, **31**, 1695–1697.
66 M. Parrinello, *J Appl Phys*, 1981, **52**, 7182–90.
67 T. Darden, D. York and L. Pedersen, *J Chem Phys*, 1993, **98**, 10089–92.
68 U. Essmann, L. Perera, M. L. Berkowitz, T. Darden, H. Lee and L. G. Pedersen, *J Chem Phys*, 1995, **103**, 8577–8593.
69 S. Páll and B. Hess, *Comput Phys Commun*, 2013, **184**, 2641–2650.
70 S. Miyamoto and P. A. Kollman, *J Comput Chem*, 1992, **13**, 952–962.
71 B. Hess, H. Bekker, H. J. Berendsen and J. G. E. M. Fraaije, *J Comput Chem*, 1997, **18**, 1463–1472.
72 B. Hess, *J Chem Theory Comput*, 2008, **4**, 116–122.
73 J. W. Polli, S. A. Wring, J. E. Humphreys, L. Huang, J. B. Morgan, L. O. Webster and C. S. Serabjit-Singh, *J Pharmacol Exp Ther*, 2001, **299**, 620–8.
74 J. Rautio, J. E. Humphreys, L. O. Webster, A. Balakrishnan, J. P. Keogh, J. R. Kunta, C. J. Serabjit-Singh and J. W. Polli, *Drug Metab Dispos*, 2006, **34**, 786–792.
75 R. Didziapetris, P. Japertas, A. Avdeef and A. Petrauskas, *J Drug Target*, 2003, **11**, 391–406.
76 K. M. M. Doan, J. E. Humphreys, L. O. Webster, S. A. Wring, L. J. Shampine, C. S. Serabjit-Singh, K. K. Adkison and J. W. Polli, *J Pharmacol Exp Ther*, 2002, **303**, 1029–1037.
77 C. Chen, E. Hanson, J. W. Watson and J. S. Lee, *Drug Metab Dispos*, 2003, **31**, 312–318.
78 A. Collett, N. B. Higgs, E. Sims, M. Rowland and G. Warhurst, *J Pharmacol Exp Ther*, 1999, **288**, 171–8.
79 K. Lee, C. Ng, K. L. R. Brouwer and D. R. Thakker, *J Pharmacol Exp Ther*, 2002, **303**, 574–580.
80 T. Tsuruo, H. Lida, S. Tsukagoshi and Y. Sakurai, *Cancer Res*, 1981, **41**, 1967–1972.
81 A. R. Safa, R. K. Stern, K. Choi, M. Agresti, I. Tamai, N. D. Mehta and I. B. Roninson, *Proc Natl Acad Sci U S A*, 1990, **87**, 7225–9.
82 B. Nare, R. K. Prichard and E. Georges, *Mol Pharmacol*, 1994, **45**, 1145–52.
83 G. A. Altenberg, C. G. Vanoye, J. K. Horton, L. Reuss and K. Julie, *Proc Natl Acad Sci U S A*, 1994, **91**, 4654–4657.
84 A. B. Shapiro, A. B. Corder and V. Ling, *Eur J Biochem*, 1997, **250**, 115–21.
85 M. Susanto and L. Z. Benet, *Pharm Res*, 2002, **19**, 457–462.
86 N. Duarte, A. Járdánházy, J. Molnár, A. Hilgeroth and M.-J. U. Ferreira, *Bioorgan Med Chem*, 2008, **16**, 9323–9330.
87 C. Vieira, N. Duarte, M. A. Reis, G. Spengler, A. M. Madureira, J. Molnár and M.-J. U. Ferreira, *Bioorgan Med Chem*, 2014, **22**, 6392–6400.
88 P. Mistry, a J. Stewart, W. Dangerfield, S. Okiji, C. Liddle, D. Bootle, J. a Plumb, D. Templeton and P. Charlton, *Cancer Res*, 2001, **61**, 749–58.
89 G. Conseil, H. Baubichon-Cortay, G. Dayan, J.-M. Jault, D. Barron, A. Di Pietro and A. Di Pietro, *Proc Natl Acad Sci U S A*, 1998, **95**, 9831–9836.
90 ChemAxon, 2012.
91 W. Humphrey, A. Dalke and K. Schulten, *J Mol Graph*, 1996, **14**, 33–38.
92 M. Mezei, *Mol Simulat*, 1989, **3**, 301–313.
93 D. van der Spoel, P. J. van Maaren, P. Larsson and N. Timneanu, *J*

Phys Chem B, 2006, **110**, 4393–8.
94 C. Blau and H. Grubmuller, *Comput Phys Commun*, 2013, **184**, 2856–2859.
95 W. J. Allen, J. A. Lemkul and D. R. Bevan, *J Comput Chem*, 2009, **30**, 1952–8.
96 G. J. Kleywegt and T. A. Jones, *Acta Crystallogr D Biol Crystallogr*, 1994, **50**, 178–85.
97 M. G. Rossmann and E. Arnold, Eds., *International Tables for Crystallography*, International Union of Crystallography, Chester, England, 2006, vol. F.
98 S. Mondal, G. Khelashvili, J. Shan, O. S. Andersen and H. Weinstein, *Biophys J*, 2011, **101**, 2092–101.
99 A. Saija, F. Bonina, D. Trombetta, A. Tomaino, L. Montenegro, P. Smeriglio and F. Castelli, *Int J Pharm*, 1995, **124**, 1–8.
100 E. K. Rooney, M. G. Gore and A. G. Lee, *Biochem Pharmacol*, 1979, **28**, 2199–2205.
101 J. W. Polli, J. L. Jarrett, S. D. Studenberg, J. E. Humphreys, S. W. Dennis, K. R. Brouwer and J. L. Woolley, *Pharm Res*, 1999, **16**, 1206–12.
102 T. Litman, T. Skovsgaard and W. D. Stein, *J Pharmacol Exp Ther*, 2003, **307**, 846–53.
103 P. Aänismaa, E. Gatlik-Landwojtowicz and A. Seelig, *Biochemistry*, 2008, **47**, 10197–207.
104 R. Kumari, R. Kumar and A. Lynn, *J Chem Inf Model*, 2014, **54**, 1951–1962.
105 A. T. García-Sosa, C. Hetényi and U. Maran, *J Comput Chem*, 2010, **31**, 174–84.
106 C. Abad-Zapatero, *Expert Opin Drug Discov*, 2007, **2**, 469–488.
107 I. K. Pajeva, M. Hanl and M. Wiese, *ChemMedChem*, 2013, **8**, 748–762.
108 N. Subramanian, K. Condic-Jurkic, A. E. Mark and M. L. O'Mara, *J Chem Inf Model*, 2015, (Article ASAP, doi: 10.1021/ci5007382).
109 T. W. Loo and D. M. Clarke, *J Biol Chem*, 2015, jbc.M115.652602.
110 T. W. Loo and D. M. Clarke, *Biochemistry*, 2013.
111 T. Kwan and P. Gros, *Biochemistry*, 1998, **37**, 3337–50.
112 R. J. Ferreira, D. J. V. A. dos Santos and M.-J. U. Ferreira, *Futur. Med Chem*, 2015, **7**, 929–946.
113 Y. Romsicki and F. J. Sharom, *Eur J Biochem*, 1998, **256**, 170–178.
114 Y. Romsicki and F. J. Sharom, *Biochemistry*, 1997, **36**, 9807–15.
115 P. Lu, R. Liu and F. J. Sharom, *Eur J Biochem*, 2001, **268**, 1687–1697.
116 S. Meyer dos Santos, C.-C. Weber, C. Franke, W. E. Müller and G. P. Eckert, *Biochem Biophys Res Commun*, 2007, **354**, 216–21.
117 S. Modok, C. Heyward and R. Callaghan, *J Lipid Res*, 2004, **45**, 1910–8.
118 P. Scheiffele, M. G. Roth and K. Simons, *EMBO J*, 1997, **16**, 5501–5508.
119 M. S. Bretscher and S. Munro, *Science (80-.).*, 1993, **261**, 1280–1281.
120 V. A. Oleinikov, F. Fleury, A. Ianoul, S. Zaitsev and I. Nabiev, *FEBS Lett*, 2006, **580**, 4953–8.
121 J. Shan, G. Khelashvili, S. Mondal and H. Weinstein, *Biophys J*, 2011, **100**, 254a.
122 S. Orlowski, S. Martin and A. Escargueil, *Cell Mol Life Sci*, 2006, **63**, 1038–1059.
123 K. Klappe, I. Hummel, D. Hoekstra and J. W. Kok, *Chem Phys Lipids*, 2009, **161**, 57–64.
124 J. Marcoux, S. C. Wang, A. Politis, E. Reading, J. Ma, P. C. Biggin, M. Zhou, H. Tao, Q. Zhang, G. Chang, N. Morgner and C. V. Robinson, *Proc Natl Acad Sci USA*, 2013, **110**, 9704–9709.
125 V. H. Teixeira, D. Vila-Viçosa, A. M. Baptista and M. Machuqueiro, *J Chem Theory Comput*, 2014, **10**, 2176–2184.
126 G.R. Marshal. *J Comput Aided Mol Des*, 2013, **27**, 107–114.
127 G.A. Cisneros, S. N.-I. Tholander, O. Parisel, T. A. Darden, D. Elking, L. Perera, J.-P. *Int. J. Quantum Chem.* 2008, **108**, 1905–1912.
128 C. Sagui, L. G. Petersen, T. A. Darden. *J Chem Phys.* 2004, **120**, 73-87.
129 Y. Shi, Z. Xia, J. Zhang,R. Best, C. Wu, J. W. Ponder, P. Ren. *J Chem Theory Comput.* 2013, **9**, 4046–4063.
130 P. Ren, C. Wu, J. W. Ponder. *J Chem Theory Comput.* 2011, **7**, 3143–3161.